

organic carbon would thus be degraded at a rate of $(0.88 \text{ to } 1.50) \times 10^{-4} \text{ gC cm}^{-3} \text{ year}^{-1}$. As a consequence, even sapropels consisting entirely of organic carbon ($\sim 0.9 \text{ gC cm}^{-3}$) would be completely degraded within 10,000 years. Organic carbon compounds in sapropels have been preserved over much longer time intervals, although a high fraction of microbial cells in the sapropels are physiologically active and continue to use organic carbon originating from the sapropels. The above comparison thus indicates that prokaryotes in sapropels have significantly lower maintenance energy requirements than any of the pure cultures investigated to date.

Mediterranean sapropels harbor large populations of previously unknown members of the green nonsulfur bacteria and crenarchaeota. Our cumulative evidence suggests that these prokaryotes are physiologically active, are specifically adapted to the specific conditions as they prevail in sediments with large amounts of subfossil kerogen, and are capable of altering the organic matter in situ even 217,000 years after its deposition.

References and Notes

1. R. J. Parkes, B. A. Cragg, P. Wellsbury, *Hydrogeology J.* **8**, 11 (2000).
2. A. E. Aksu, T. Abrajano, P. J. Mudie, D. Yasar, *Mar. Geol.* **153**, 303 (1999).
3. R. B. Kidd, M. B. Cita, W. B. F. Ryan, *Init. Rep. Deep Sea Drill. Proj.* **42A**, 421 (1978), K. J. Hsü et al., Eds.
4. W. B. F. Ryan, M. B. Cita, *Mar. Geol.* **23**, 197 (1977).
5. H. L. Ten Haven, M. Baas, J. W. De Leeuw, P. A. Schenk, *Mar. Geol.* **75**, 137 (1987).
6. Materials and methods and supplementary figures are available as supporting material on Science Online.
7. G. Ruddy, in *Biogeochemistry of Intertidal Sediments*, T. D. Jickells, J. E. Rae, Eds. (Cambridge Univ. Press, Cambridge, 1997), pp. 99–118.
8. R. J. Chróst, in *Microbial Enzymes in Aquatic Environments*, R. J. Chróst, Ed. (Springer, New York, 1991), pp. 29–57.
9. J. Overmann, J. T. Beatty, K. J. Hall, *Appl. Environ. Microbiol.* **62**, 3251 (1996).
10. M. J. L. Coolen, J. Overmann, *Appl. Environ. Microbiol.* **66**, 2589 (2000).
11. A. Boetius, E. Damm, *Deep-Sea Res.* **45**, 239 (1998).
12. A. Boetius, S. Scheibe, A. Tselepidis, H. Thiel, *Mar. Ecol. Prog. Ser.* **140**, 239 (1996).
13. K. Poremba, H. G. Hoppe, *Mar. Ecol. Prog. Ser.* **118**, 237 (1995).
14. S. T. Petsch, T. I. Eglinton, K. J. Edwards, *Science* **292**, 1127 (2001).
15. R. G. Keil, D. B. Montluçon, F. G. Prahl, J. I. Hedges, *Nature* **370**, 549 (1994).
16. K. A. Bidle, M. Kastner, D. H. Bartlett, *FEMS Microbiol. Lett.* **177**, 101 (1999).
17. R. J. Parkes et al. *Nature* **371**, 410 (1994).
18. M. J. L. Coolen, J. Overmann, *Appl. Environ. Microbiol.* **64**, 4513 (1998).
19. C. Vetriciani, H. W. Jannasch, B. J. MacGregor, D.A. Stahl, A.-L. Reysenbach, *Appl. Environ. Microbiol.* **65**, 4375 (1999).
20. X. Maymó-Gatell, Y.-T. Chien, J. M. Gossett, S. H. Zinder, *Science* **276**, 1568 (1997).
21. Y. Sekiguchi, H. Takahashi, Y. Kamagata, A. Ohashi, H. Harada, *Appl. Environ. Microbiol.* **12**, 5740 (2001).
22. P. Hugenholtz, B. M. Goebel, N. R. Pace, *J. Bacteriol.* **180**, 4765 (1998).
23. D. P. Chandler, F. J. Brockman, T. J. Bailey, J. K. Fredrickson, *Microb. Ecol.* **36**, 37 (1998).

24. J. C. M. Scholten, R. Conrad, *Appl. Environ. Microbiol.* **66**, 2934 (2000).
25. S. Norland, in *Handbook of Methods in Aquatic Microbial Ecology*, P. F. Kemp, B. F. Sherr, E. B. Sherr, J. J. Cole, Eds. (Lewis Publishers, Boca Raton, FL, 1993), pp. 303–307.
26. K. Zengler, H. H. Richnow, R. Rosselló-Mora, W. Michaelis, F. Widdel, *Nature* **401**, 266 (1999).
27. We thank the master and the crew of the RV *Meteor* and our colleagues on board for their help during collection of the sediment cores and G. Muyzer and

M. Overeijnder of the Kluwer Laboratory, TU-Delft, for help with real-time PCR. Supported by grants of the Deutsche Forschungsgemeinschaft to J.O. and H.C. (DFG Cy 1/8-1 and 1/10-1).

Supporting Online Material

www.sciencemag.org/cgi/content/full/296/5577/2407/DC1
Materials and Methods
Figs. S1 to S3

14 March 2002; accepted 17 May 2002

Correction of ADA-SCID by Stem Cell Gene Therapy Combined with Nonmyeloablative Conditioning

Alessandro Aiuti,¹ Shimon Slavin,² Memet Aker,² Francesca Ficara,¹ Sara Deola,¹ Alessandra Mortellaro,¹ Shoshana Morecki,² Grazia Andolfi,¹ Antonella Tabucchi,³ Filippo Carlucci,³ Enrico Marinello,³ Federica Cattaneo,¹ Sergio Vai,¹ Paolo Servida,⁴ Roberto Miniero,⁵ Maria Grazia Roncarolo,^{1,6} * Claudio Bordignon^{1,6,*} †

Hematopoietic stem cell (HSC) gene therapy for adenosine deaminase (ADA)-deficient severe combined immunodeficiency (SCID) has shown limited clinical efficacy because of the small proportion of engrafted genetically corrected HSCs. We describe an improved protocol for gene transfer into HSCs associated with nonmyeloablative conditioning. This protocol was used in two patients for whom enzyme replacement therapy was not available, which allowed the effect of gene therapy alone to be evaluated. Sustained engraftment of engineered HSCs with differentiation into multiple lineages resulted in increased lymphocyte counts, improved immune functions (including antigen-specific responses), and lower toxic metabolites. Both patients are currently at home and clinically well, with normal growth and development. These results indicate the safety and efficacy of HSC gene therapy combined with nonmyeloablative conditioning for the treatment of SCID.

Gene therapy trials have demonstrated the safety and feasibility of engineering hematopoietic stem cells (HSCs) for treating inherited hematopoietic diseases (1–6). In these studies, however, the frequency of multipotent genetically modified HSCs and the levels of long-term transgene expression were variable, with limited clinical effect. This variability could be influenced by vector design, gene transfer protocols, or inadequate engraftment and expansion of genetically corrected HSCs. Recent improvements in HSC gene transfer, combined with a strong selec-

tive advantage for growth and differentiation of lymphoid cells, allowed investigators to correct the immune defect in the SCID variant due to γ -chain deficiency (SCID-X1) (7).

In ADA-SCID the purine metabolic defect (8) leads primarily to impaired lymphocyte development and function but also to nonimmunological abnormalities, which indicates that this disease is more complex than other SCIDs (8–10). The accumulation of toxic metabolites may offer a selective advantage to cells that produce sufficient vector-derived ADA. In previous gene therapy trials, this advantage might have been lost because of simultaneous treatment with bovine enzyme [polyethylene glycol-conjugated ADA (PEG-ADA)] replacement therapy. Recent experience with an ADA-SCID patient treated with transduced peripheral blood lymphocytes (PBL) (11, 12) shows that PEG-ADA discontinuation results in preferential expansion of T cells containing the ADA gene capable of sustaining immune functions, but it did not completely correct the metabolic defect (12). These data suggest that, for long-term full

¹San Raffaele Telethon Institute for Gene Therapy (HSR-TIGET), Milan, Italy. ²Departments of Bone Marrow Transplantation and Pediatrics, Hadassah University Hospital, Jerusalem, Israel. ³Institute of Biochemistry and Enzymology, University of Siena, Siena, Italy. ⁴BMT and Gene Therapy Program, Scientific Institute H. S. Raffaele; ⁵Department of Biological and Clinical Science, University of Turin, Turin, Italy. ⁶Università Vita-Salute San Raffaele, Milan, Italy.

*These authors contributed equally to this work.

†To whom correspondence should be addressed. E-mail: claudio.bordignon@hsr.it

clinical benefit, correcting the metabolic defect could be as important as correcting the immune defect.

We recently developed an improved gene transfer protocol into CD34⁺ HSCs (13–15), which allows efficient transduction while preserving differentiation capacity into multiple lineages, including myeloid cells, B cells, natural killer (NK) cells, and T lymphocytes, as shown by in vitro and in vivo assays (15). We applied this protocol to two ADA-SCID patients (Pt1 and Pt2), who lacked an HLA-identical sibling donor and for whom PEG-ADA was not available (13). To provide an initial developmental advantage to transduced HSCs and create space in the bone marrow (BM), we treated the patients with a low-intensity, nonmyeloablative conditioning regimen (13). This allowed us to fully exploit the selective advantage of genetically corrected cells and to evaluate the clinical efficacy of gene therapy.

Pt1 and Pt2 were enrolled in the gene therapy trial at 7 months and at 2 years and 6 months of age, respectively (13). Autologous CD34⁺ cells were collected from BM (Pt1, 4.15 × 10⁶ cells per kg of body weight; Pt2, 1.08 × 10⁶ cells per kg of body weight), transduced with GIAD1 retroviral vector, and infused 4 days later (13). Pt1 received 8.6 × 10⁶ CD34⁺ cells per kg, containing 25% transduced colony-forming units in culture (CFU-C), and Pt2 received 0.9 × 10⁶ CD34⁺ cells per kg, with 21% transduced CFU-C. At days -3 and -2, both patients received nonmyeloablative conditioning with busulfan (2 mg per kg per day). Neither patient experienced toxicity nor required blood component transfusion. After a transient myelosuppression (neutrophil nadir: Pt1, day +17, 0.15 × 10³ cells per μl; Pt2, day +19, 0.4 × 10³ cells per μl; platelet nadir: Pt1, day +31, 154 × 10³ cells per μl; Pt2, day +30, 23 × 10³ cells per μl), hematopoiesis recovered as expected [days to absolute neutrophil count (ANC) ≥ 500 cells per μl: Pt1, 22 days; Pt2, 21 days] (Fig. 1, A and B). Pt1, whose pretreatment ANC was already low, experienced 12 days of ANC < 500 and then recovered to normal levels (Fig. 1A), whereas Pt2 experienced a single day of ANC < 500 (Fig. 1B). In Pt1, who has a follow-up of 14 months, the number of PBL increased progressively from <100 per μl to 2000 per μl at day +150, a level that was maintained throughout the remaining follow-up (Fig. 1C). Within the lymphocyte subsets, the first increase occurred in B cells and NK cells, followed by T cells (day +90) (Fig. 1E) (13). T cells developed normally into both CD3⁺/CD4⁺ cells and CD3⁺/CD8⁺ subsets (Fig. 1G) and expressed a normal pattern of activation markers. Restoration of thymic activity was demonstrated by the dramatic increase in CD4⁺/CD45RA⁺ naive T cells and

T cell receptor excision circles (TREC) (16) in CD3⁺ cells to the levels observed in age-matched controls (Fig. 1G) (13). Gene therapy led to normalization of proliferative responses to polyclonal stimuli [CD3 monoclonal antibody (anti-CD3 mAb), with or without anti-CD28 mAb, phytohemagglutinin (PHA), pokeweed mitogen, and concanavalin A] and, more importantly, to nominal antigens (candida, tetanus toxoid) (Fig. 2A) (13, 17). Proliferative responses and cytotoxic activity to alloantigens were normal. The T cell receptor variable region β chain repertoire evaluated by polymerase chain reaction (PCR) heteroduplex analysis (18) showed a normal heterogeneous pattern. Serum immunoglobulin M (IgM), immunoglobulin A (IgA), and immunoglobulin G (IgG) increased to normal levels, which allowed us to discontinue intravenous immunoglobulin (IVIG) 6 months after gene therapy (Fig. 2A), and we detected isohemagglutinins for the first time (1:8 to 1:16). After vaccination with tetanus toxoid, both T cell proliferative responses and specific antibody levels in the serum were comparable to those of age-matched controls (Fig. 2A). A follow-up of 12 months is available for Pt2. In this patient, lymphocytes increased to 400 cells per μl,

with slower kinetics than Pt1 (Fig. 1D). The increase occurred mostly in the T cell subset (Fig. 1F), as indicated by a significant increase in TREC (Fig. 1H). Gene therapy led to a substantial increase in proliferative responses to polyclonal stimuli (Fig. 2B). T cell lines generated ex vivo 6 months after gene therapy proliferated normally in response to interleukin 2 and anti-CD3 mAb, with or without anti-CD28 mAb.

Several findings support the hypothesis that Pt2 is also reconstituting B cell functions: (i) normalization of serum IgM and IgA was achieved by the fourth month after gene therapy (Fig. 2B); (ii) the patient maintained IgG levels above 800 mg/dl in response to a delayed schedule of IVIG, which suggests endogenous IgG production; (iii) before gene therapy and despite IVIG, the patient was affected by recurrent respiratory infections, chronic diarrhea, and scabies. Twelve months after gene therapy, the patient showed no sign of respiratory infections and scabies and recovered normally from two transient episodes of diarrhea.

We next analyzed by quantitative real-time PCR (Q-PCR) (13) the proportion of vector-containing cells in purified subpopulations of PB and BM from both patients at

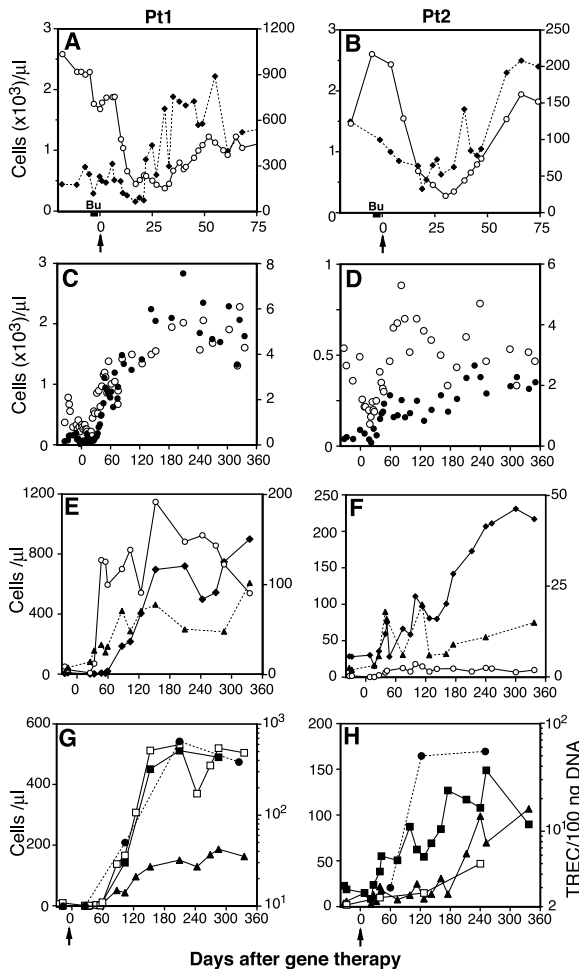


Fig. 1. Hematopoietic and lymphoid reconstitution after gene therapy. (A and B) Absolute neutrophil counts (solid diamonds) and platelet counts (open circles) (right ordinate) of Pt1 (left column) and Pt2 (right column) before and after gene therapy. Bu indicates the 2 days of busulfan administration; arrows show the date of infusion of transduced CD34⁺ cells (day 0). (C and D) Total lymphocyte counts (solid circles) (left ordinate) and white blood cell counts (open circles) (right ordinate) in the PB. (E and F) Absolute counts of PB CD19⁺ B cells (open circles), CD3⁺ T cells (solid diamonds) (left ordinate), and CD56⁺/CD16⁺ NK cells (solid triangles) (right ordinate). (G and H) Absolute counts of PB CD3⁺/CD4⁺ T cells (solid squares), CD3⁺/CD8⁺ T cells (solid triangles), CD4⁺/CD45RA⁺ naive T cells (open squares), and numbers of TREC (solid circles) in CD3⁺ cells. The scale for TREC numbers is on the right. TREC levels in age-matched controls are 270 ± 130 copies per 100 ng of DNA.

REPORTS

different time points after gene therapy (Fig. 3). Vector-containing cells were detected first in granulocytes as early as 3 weeks in Pt1 and at 2 weeks in Pt2. Both patients showed genetically corrected cells in multiple lineages, including granulocytic, erythroid, megakaryocytic, and lymphoid cells, which were detected at higher levels in Pt1. The frequency of vector-containing cells was higher in lymphoid subsets (Fig. 3, C, D, G, and H) than in the other lineages (Fig. 3, A, B, E, and F), which indicates a stronger selective advantage for differentiation of genetically corrected B, NK, and T cells. We also observed an initial increase in untransduced cells (in Pt1 from 10 CD3⁺ cells per μ l before gene therapy to 220 cells per μ l at day 100, with 70% untransduced cells), which could be related to a beneficial effect of systemic detoxification mediated by ADA-producing transduced cells.

In Pt1, the frequency of vector-containing T cells increased progressively and reached 70% at 11 months of follow-up (Fig. 3C). At the same time, virtually all NK cells present in PB and in BM were transduced (Fig. 3C). Transduced B cells were first detected in the BM at day +30 and 1 month later in PB (Fig. 3D). Strikingly, the frequency of transduced B cells was higher in the PB than in the BM, which suggests a preferential differentiation of genetically corrected cells and/or a growth advantage for peripheral B cells. The observation that BM immature B cells (surface IgM⁺) contained a higher frequency of transduced cells (17%) than pre-B cells (8.5%) confirmed this hypothesis. In Pt2, genetically engineered CD3⁺ T cells appeared later than in Pt1, but the frequency of these cells progressively increased up to 100% at day +240 (Fig. 3G). Persistent production of genetically corrected granulocytes, monocytes, megakaryocytes, and erythroid cells was observed, with levels ranging from 5 to 20% (Fig. 3, A and B) in Pt1, demonstrating the engraftment of multipotent HSCs. This conclusion was further supported by the consistent finding of neomycin (Neo)-resistant CFU-C (6.5% at day +330), which was confirmed by PCR analysis of individual CFU-C and by Q-PCR of purified BM CD34⁺ cells (11% at day +330) (Fig. 3A).

To prove that genetically corrected HSCs retained their repopulation and differentiation properties, we isolated CD34⁺ cells from the BM of Pt1 at day +330 after gene therapy and tested them for their lymphoid differentiation capacity. CD34⁺ cells plated in vitro into a B/NK differentiation assay were able to generate B and NK cells that contained 4 and 9% of transduced cells, respectively (15). BM CD34⁺ cells were also transplanted into the BM/thymus of SCID-hu mice (19) and analyzed after 8 weeks. Donor cells (identified by HLA-specific mAb) engrafted in the BM/

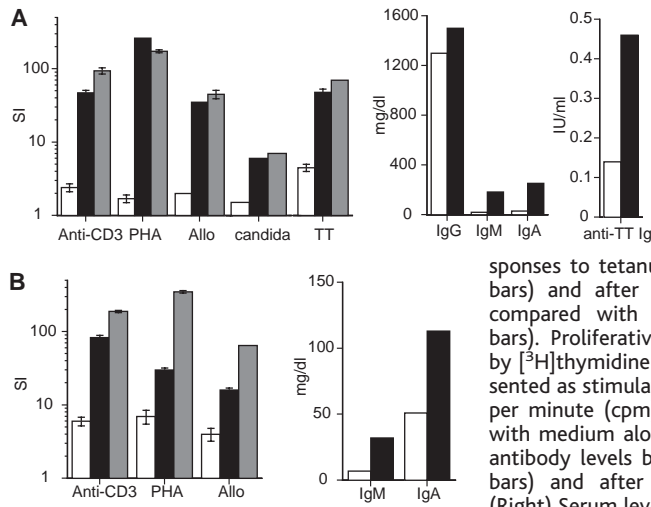


Fig. 2. Restoration of immune functions. (A) Pt1. (Left) Proliferative responses to anti-CD3 mAb, PHA, alloantigen, and candida stimuli before (open bars) and after (solid bars) gene therapy, compared with age-matched control (gray bars). Proliferative responses to tetanus toxoid (TT) before (open bars) and after (solid bars) vaccination are compared with age-matched control (gray bars). Proliferative responses were evaluated by [³H]thymidine incorporation and are represented as stimulation index [SI, ratio of counts per minute (cpm) with the stimuli over cpm with medium alone] (13, 25). (Middle) Serum antibody levels before (while on IVIG) (open bars) and after (solid bars) gene therapy. (Right) Serum levels of antibody specific to TT

before (open bars) and after (solid bars) vaccination with TT. Patient was vaccinated 3 months after discontinuation of IVIG. Protective values for anti-TT antibodies are >0.1 international unit/ml. (B) Pt2. (Left) Proliferative responses to anti-CD3, PHA, and alloantigen stimuli before (open bars) and after (solid bars) gene therapy, compared with age-matched control (gray bars). (Right) Serum immunoglobulin levels before (open bars) and after (solid bars) gene therapy.

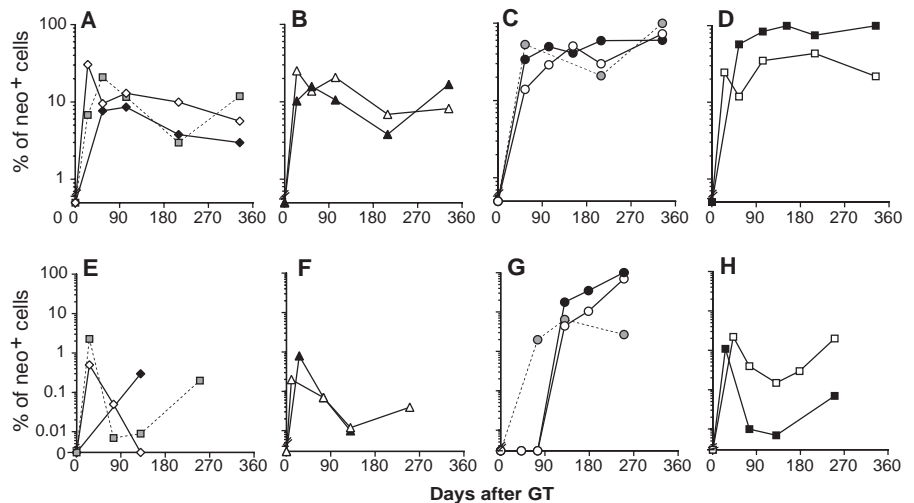


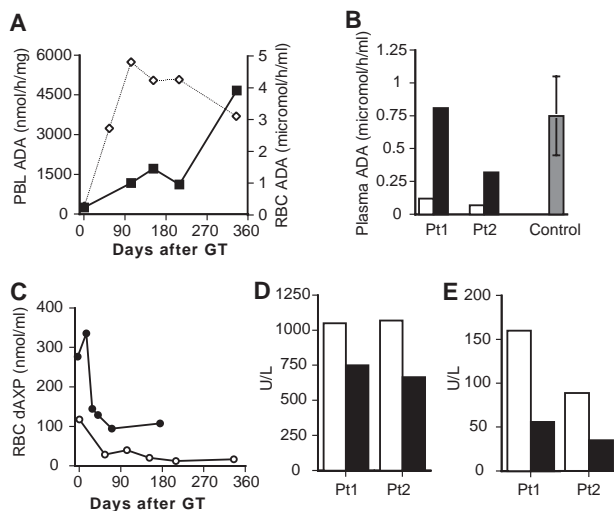
Fig. 3. Quantitative PCR analysis for vector-containing cells. Cells were sorted by flow cytometry (13, 26). DNA was isolated and analyzed by real-time Q-PCR analysis (13) for the proportion of vector-positive (Neo⁺) cells in Pt1 (A to D) and Pt2 (E to H). Graphs show percent of Neo⁺ cells in the following sorted cell populations: (A and E) CD34⁺ progenitor cells (gray squares), CD61⁺ megakaryocytic cells (solid diamonds), and glycophorin A⁺ erythroid cells (open diamonds) from the BM; (B and F) CD15⁺ granulocytic cells from the BM (open triangles) or the PB (solid triangles); (C and G) CD3⁺ T cells (open circles), CD56⁺/CD16⁺ NK cells (gray circles) and T-cell lines (solid circles) from the PB; (D and H) CD19⁺ B cells from the BM (open boxes) or the PB (solid boxes).

thymus and differentiated into transduced mature B and T cells (frequency of transduced CD19⁺ cells by Q-PCR, range 0.3 to 15.2%; CD3⁺ cells, range 0.14 to 31.2%). These data formally demonstrate that engineered HSCs retained their ability to reconstitute human hematolymphopoiesis in vitro and in vivo in a secondary transplant 11 months after infusion.

Biochemical studies (13, 20) demonstrated that gene therapy completely restored intracellular ADA enzymatic activity in PBL (Fig. 4A) and in BM CD19⁺ B cells (590

units versus 300 ± 100 units in normal controls). Indeed, vector ADA was expressed at the mRNA level in differentiated cells of Pt1, as assessed by reverse transcriptase (RT)-PCR analysis in T cells, B cells, granulocytes, and monocytes (17). In erythrocytes (RBCs), enzyme activity increased from undetectable to 20 to 30% of healthy controls (Fig. 4A) and was detectable in myeloid progenitors differentiated in vitro (CFU-GM) (550 units; normal values, 5000 ± 2000 units). In Pt2, BM ADA activity increased eightfold (from 180 to 1500 units) after gene

Fig. 4. Biochemical studies for ADA and purine metabolites. **(A)** Intracellular ADA activity in PBL (solid boxes) (units expressed as nmol·hour⁻¹·mg⁻¹) and in RBC (open diamonds) (units expressed as μmol·hour⁻¹·ml⁻¹) of Pt1. Normal ADA activity in PBL: 1350 ± 650 nmol hour⁻¹ mg⁻¹. Normal ADA activity in RBC: 12 ± 2 μmol hour⁻¹ ml⁻¹. Two and a half months before gene therapy Pt1 received an exchange transfusion of RBC, which might have reduced the initial dAXP value. **(B)** ADA activity in plasma of Pt1 and Pt2 before (open bars) and after (solid bars) gene therapy and in age-matched controls (gray bars) (units expressed as μmol of plasma per hour per ml). Normal ADA activity in plasma: 0.7 ± 0.3 units. **(C)** Concentration of dAXP purine metabolites in RBC, measured at different time points of follow-up in Pt1 (open circles) and Pt2 (solid circles), expressed as nmol/ml. Normal values: 0 nmol/ml. **(D)** Serum levels of LDH in Pt1 and Pt2 before (open bars) and after (solid bars) gene therapy (normal LDH values, 300 to 600 units/liter). **(E)** Serum levels of aspartate aminotransferase (AST) before (open bars) and after (solid bars) gene therapy (normal AST values, 2 to 60 units/liter).



therapy. ADA activity in the plasma increased in both patients after gene therapy (Fig. 4B). This increase was paralleled by a decline in RBC toxic adenine deoxyribonucleotide (dAXP) metabolites to levels equal to 10 and 40% of the initial value for Pt1 and Pt2, respectively—levels comparable to those found in patients successfully transplanted with allogeneic BM (21, 22) (Fig. 4C). The amelioration of the metabolic pattern was followed by a normalization of lactate dehydrogenase (LDH) and liver enzymes usually elevated in ADA-SCID (8, 9) (Fig. 4, D and E). During this follow-up, the two patients were in good clinical condition and did not experience any severe infectious episodes. Both patients are currently at home and clinically well, with normal growth and development. They live a normal life in their native countries and remain off enzyme replacement therapy.

Several explanations may account for the different levels of engraftment of transduced cells and restoration of the immune functions in these two patients. First, Pt2 received one log (one order of magnitude) lower autologous transduced CD34⁺ cells than Pt1. Second, Pt2 was enrolled at an older age, which can be a crucial factor for HSC engraftment,

as shown in BMT transplantation in SCID (23). An additional, and possibly more important, variable may be the degree of host BM ablation. Indeed, the pharmacologic biodistribution of busulfan might have differed in the two patients, because Pt1 received the drug intravenously and Pt2 received it orally. These results suggest that early intervention with optimal amounts of transduced HSCs and adequate conditioning are crucial factors in determining the speed and level of engraftment.

A similar gene transfer protocol was used to transduce BM CD34⁺ cells of two SCID-X1 patients (7) without conditioning. In this study, gene therapy resulted in the development of T and NK corrected cells, allowing full reconstitution of T cell functions, whereas B lymphocytes and other hematopoietic cells remained mostly untransduced. The use of conditioning is most likely responsible for the improved results of our protocol, and this advantage may counteract the toxic effects and potential complications associated with low-dose busulfan.

Overall, our results prove the safety and efficacy of HSC gene therapy combined with nonmyeloablative conditioning in restoring lymphoid development and functions and in

correcting the metabolic defect of ADA-SCID with complete reversal of the clinical phenotype, in the absence of enzyme replacement. These results represent a significant advance over the pioneering studies of gene therapy with PBL in ADA-SCID patients receiving PEG-ADA that showed efficient gene transfer into long-living T lymphocytes (1, 24).

References and Notes

1. C. Bordignon et al., *Science* **270**, 470 (1995).
2. D. B. Kohn et al., *Nature Med.* **1**, 1017 (1995).
3. P. M. Hoogerbrugge et al., *Gene Ther.* **3**, 179 (1996).
4. D. B. Kohn et al., *Nature Med.* **4**, 775 (1998).
5. H. L. Malech et al., *Proc. Natl. Acad. Sci. U.S.A.* **94**, 12133 (1997).
6. T. R. Bauer Jr., D. D. Hickstein, *Curr. Opin. Mol. Ther.* **2**, 383 (2000).
7. M. Cavazzana-Calvo et al., *Science* **288**, 669 (2000).
8. R. Hirschhorn, in *Primary Immunodeficiency Diseases*, H. Ochs, C. Smith, J. Puck, Eds. (Oxford Univ. Press, Oxford, 1999), pp. 121–139.
9. M. E. Bollinger et al., *N. Engl. J. Med.* **334**, 1367 (1996).
10. M. H. Rogers, R. Lwin, L. Fairbanks, B. Gerritsen, H. B. Gaspar, *J. Pediatr.* **139**, 44 (2001).
11. C. Bordignon et al., *Hum. Gene Ther.* **4**, 513 (1993).
12. A. Aiuti et al., *Nature Med.* **8**, 423 (2002).
13. Materials and methods are available as supporting material on Science Online.
14. J. S. Dando, A. Aiuti, S. Deola, F. Ficara, C. Bordignon, *J. Gene Med.* **3**, 219 (2001).
15. F. Ficara et al., unpublished observations.
16. L. Zhang et al., *J. Exp. Med.* **190**, 725 (1999).
17. A. Aiuti et al., unpublished data.
18. A. Wack, D. Montagna, P. Dellabona, G. Casorati, *J. Immunol. Methods* **196**, 181 (1996).
19. M. G. Roncarolo, J. M. Carballido, M. Rouleau, R. Namikawa, J. E. de Vries, *Semin. Immunol.* **8**, 207 (1996).
20. F. Carlucci et al., *Electrophoresis* **21**, 1552 (2000).
21. R. Hirschhorn, M. V. Roegner, L. Kuritsky, F. S. Rosen, *J. Clin. Invest.* **68**, 1387 (1981).
22. H. D. Ochs et al., *Blood* **80**, 1163 (1992).
23. R. H. Buckley et al., *N. Engl. J. Med.* **340**, 508 (1999).
24. R. M. Blaese et al., *Science* **270**, 475 (1995).
25. R. Bacchetta et al., *J. Exp. Med.* **179**, 493 (1994).
26. A. Aiuti et al., *Blood* **94**, 62 (1999).
27. We thank the nurses in the BMT and Gene Therapy Program Department of Hematology at the Scientific Institute H. S. Raffaele and at Hadassah University for skilled and dedicated care. We thank S. Yoshimura for providing CH-296 fibronectin fragment (Takara); Y. Gelfand for excellent technical assistance in handling cells of Pt1; C. Mocchetti, N. Carballido, and J. Carballido for help with SCID-hu mice; M. S. Hershfield for initial help in setting up the biochemical assays; R. Sciarretta Birolo for PCR analysis; and L. Parma and G. Torriani for flow cytometry and cell sorting. HSR-TIGET is supported by the Italian Telethon Foundation.

Supporting Online Material

www.sciencemag.org/cgi/content/full/296/5577/2410/DC1
Materials and Methods

22 January 2002; accepted 22 May 2002